Surface Functionalization of Bioactive Glasses with Polyphenols from *Padina pavonica* Algae and In Situ Reduction of Silver Ions: Physico-Chemical Characterization and Biological Response

Asmaa Sayed Abdelgeliel [1,2], Sara Ferraris [3], Andrea Cochis [1,4], Sara Vitalini [5], Marcello Iriti [5], Hiba Mohammed [1], Ajay Kumar [1], Martina Cazzola [3], Wesam M. Salem [2], Enrica Verné [3], Silvia Spriano [3] and Lia Rimondini [1,4,*]

1 Department of Health Sciences, Università del Piemonte Orientale UPO, 28100 Novara (NO), Italy; asmaa.elgafari@sci.svu.edu.eg (A.S.A.); andrea.cochis@med.uniupo.it (A.C.); hiba.mohammed@med.uniupo.it (H.M.); ajaykumar2420@gmail.com (A.K.)

2 Botany & Microbiology Department, South Valley University, Qena 83523, Egypt; wesam.salem@sci.svu.edu.eg

3 Department of Applies Science and Technology, Politecnico di Torino, 10129 Torino (TO), Italy; sara.ferraris@polito.it (S.F.); martina.cazzola@polito.it (M.C.); enrica.verne@polito.it (E.V.); silvia.spriano@polito.it (S.S.)

4 Interdisciplinary Research Center of Autoimmune Diseases (IRCAD) and Center for Translational Research on Autoimmune & Allergic Diseases-CAAD, 28100 Novara (NO), Italy

5 Department of Agricultural and Environmental Sciences, Università degli Studi di Milano, 20133 Milan (MI), Italy; sara.vitalini@unimi.it (S.V.); marcello.iriti@unimi.it (M.I.)

* Correspondence: lia.rimondini@med.uniupo.it; Tel.: +39-0321-660673

Abstract: Bioactive glasses (BGs) are attractive materials for bone replacement due to their tailorable chemical composition that is able to promote bone healing and repair. Accordingly, many attempts have been introduced to further improve BGs' biological behavior and to protect them from bacterial infection, which is nowadays the primary reason for implant failure. Polyphenols from natural products have been proposed as a novel source of antibacterial agents, whereas silver is a well-known antibacterial agent largely employed due to its broad-ranged activity. Based on these premises, the surface of a bioactive glass (CEL2) was functionalized with polyphenols extracted from the Egyptian algae *Padina pavonica* and enriched with silver nanoparticles (AgNPs) using an in situ reduction technique only using algae extract. We analyzed the composite's morphological and physical-chemical characteristics using FE-SEM, EDS, XPS and Folin–Ciocalteau; all analyses confirmed that both algae polyphenols and AgNPs were successfully loaded together onto the CEL2 surface. Antibacterial analysis revealed that the presence of polyphenols and AgNPs significantly reduced the metabolic activity (>50%) of *Staphylococcus aureus* biofilm in comparison with bare CEL2 controls. Finally, we verified the composite's cytocompatibility with human osteoblasts progenitors that were selected as representative cells for bone healing advancement.

Keywords: bioactive glass; polyphenols; silver nanoparticles; physico-chemical; antibacterial; cytocompatibility

1. Introduction

Due to the continuous increase in chronic/non-chronic etiologies resulting in different kinds of bone defects, scientists have aimed to find new strategies to promote bone tissue reconstruction via self-regenerative stimulation [1–3].

Bioactive glasses (BGs) are biocompatible materials, currently applied for rapid induction of bone tissue regeneration due to their tailorable chemical composition that is able to promote bone healing and repair. This process is promoted by BGs osteoconduction and osteoinduction properties: once a BG is introduced into the defect, an immediate and continuous dissolution of critical concentrations of soluble P, Ca, Si, and Na ions stimulates the self-renewal healing of the healthy bone surrounding the defect [4–6]. In particular, once the BG comes into contact with the physiological environment, it starts to release Na^+ and Ca^{2+} ions and to exchange H^+, thus forming a hydrated silica gel on the surface. This gel turns into an amorphous $CaO-P_2O_5-SiO_2$ layer with a continuous consumption of Ca^{2+} and PO_4^{3-}, and subsequently crystallizes into a hydroxycarbonate apatite (HCA) layer through constant incorporation with Ca^{2+}, PO_4^{3-}, OH^-, and CO_3^{2-} [7,8]. The growing HCA layer provides an ideal environment for osteoblasts colonization, proliferation, and differentiation [9,10].

As an attempt to improve the BG outcome, the addition of natural products has been considered to improve their bioactivity and prevent the surface from bacterial infection. Marine algae have been proven to have valuable impacts on therapeutics and pharmaceuticals as a natural renewable material, wealthy in a variety of bioactive compounds [11]. In particular, the algal polysaccharides, proteins, polyunsaturated fatty acids, pigments, as well as polyphenols, such as flavonoids, can serve as bioactive bases of novel medical products [12]. Amongst them, *Padina pavonica* is a famous species of Egyptian marine algae that demonstrated antioxidant properties due to its polyphenols content [13,14]. Considering that this particular alga is abundant and inexpensive in Egypt but does not currently have any application, a possible use for biomedical purposes can be considered for the improvement of the local economy and for the development of a sustainable use of resources. Previous literature demonstrated that some algal-derived phytochemicals, including polyphenols and flavonoids, exhibited antioxidant, anti-inflammatory, as well as broad-range antimicrobial activities [15]. These antioxidant activities rely on the polyphenols' potential in reducing the production of reactive oxygen species (ROS) through inhibiting oxidases, decreasing superoxide production, ameliorating the mitochondrial oxidative process, and inhibiting the formation of oxidized low-density lipoprotein [16]. From an antibacterial point of view, flavonols displayed a remarkable broad-range activity against several Gram-positive bacteria, such as *Staphylococcus aureus* as well as Gram-negative bacteria [17]. The above-mentioned antibacterial effect is due to the polyphenols' antioxidant activity that damages the cell membrane and causes leakage of the biomolecules into the bacteria cell [18–20].

Another attractive broad-range antibacterial treatment adopted as an alternative to conventional antibiotics is represented by inorganic metal ions and nanoparticles [21–24]. The principle advantages of the ions' use are their broad range activity toward both Gram-positive and Gram-negative bacteria, as well as their ability to avoid most of the resistance mechanism exploited by pathogens to counteract drug activity [24]. Amongst the large class of antibacterial metal ions, silver (Ag) is probably the most used and characterized as its wide range of antibacterial effects has been widely demonstrated [21]. In particular, when a biomaterial surface is coated by silver nanoparticles (AgNPs), these particles provide better surface contact between Ag and the microorganism. As such, the cell membrane is impaired, allowing AgNPs to invade the cell causing oxidative stress [25]. As a consequence, DNA damage, genotoxicity, and chromosomal abnormality occur, thus leading to apoptosis [26].

Based on these premises, in the present work, functionalized BG scaffolds were grafted for the first time with a combination of *Padina pavonica* extract and AgNPs using an in situ reduction technique we previously described [21]. The composite's surface chemical-physical was characterized using Folin–Ciocalteau, X-ray photoelectron spectroscopy (XPS), field emission scanning electron microscopy (FE-SEM), and energy dispersive X-ray (EDS). Then, the antibacterial activity was evaluated towards a multi-drug resistant biofilm former strain of *Staphylococcus aureus* by means of metabolic activity reduction. Finally, the composite's cytocompatibility was verified towards human osteoblasts progenitors that were selected as representative of bone cells deputies to drive the self-healing process.

2. Materials and Methods

2.1. Padina pavonica Macroalgae Selection, Collection, and Storage

Padina pavonica (P. pavonica) macroalgae were collected by hand picking from the Red Sea in Hurghada, Egypt. Then, healthy algae samples were immediately cleaned of epiphytes and extraneous matter, and necrotic algae were discarded. Specimens were washed thoroughly with sterile distilled water, air dried, cut into small pieces, and then strongly pressed in a tissue grinder until obtaining a fine powder (IKA A 10, IKA®-Werke GmbH & Co. KG, Staufen im Breisgau, Germany).

2.2. Determination of Polyphenols, Carotenoids, and Chlorophylls from P. pavonica Extract

Polyphenols were extracted and characterized from the *P. pavonica* powder using solvent technique (95% ethanol, *v/v* in ultrapure water) and the colorimetric Folin–Ciocalteau method, respectively [27–29]. Briefly, algae powder was added to the ethanol solution in a ratio of 1:50 (*w/v*); then, the solution was heated to 60 °C for 1 h under continuous stirring (120 rpm). Afterward, the solution was 0.45-μm filtered to remove unsolved debris and ethanol was fully evaporated into an incubator (60 °C, 2 h). Finally, the obtained extract was resuspended in ultrapure water, freeze-dried (using a Scanvac CoolSafe 4, from LaboGene, Lillerød, Denmark) and stored at −20 °C until use.

Total polyphenol content (TPC) of the powdered algae was determined calorimetrically by the Folin–Ciocalteau method with slight modifications. Briefly, 0.5 mL of the ethanolic solution was added to 2.5 mL of 10% Folin–Ciocalteau reagent, previously diluted with distilled water. After 3 min, 2 mL of 7.5% sodium carbonate solution was added. The mixture was incubated in the dark for 1 h at room temperature and its absorbance was measured at 765 nm using a UV-Vis spectrophotometer (Jenway 7205, Cole-Parmer, Staffordshire, UK). A calibration curve was prepared with gallic acid standard solution at various concentrations (10 to 100 mg/L). The results are expressed as mg gallic acid equivalent (GAE)/g dry weight (DW). Total carotenoid (C), chlorophyll-a (Chl-a) and chlorophyll-b (Chl-b) contents of the extracts were determined spectrophotometrically (Jenway 7205, Cole-Parmer, Staffordshire, UK) according to Sumanta et al. [28].

2.3. Specimen Preparation and Physico-Chemical Characterization

2.3.1. Specimen Preparation

The bioactive glass CEL2, with molar composition of 45% SiO_2, 3% P_2O_5, 26% CaO, 7% MgO, 15% Na_2O, and 4% K_2O, was prepared by the melt and quenching route to obtain the bulk form. Glass bars were then cut into 2-mm-thick slices and polished with SiC abrasive papers up to 4000 grit. Polished specimens were gently washed with ultrapure water prior to undergoing surface functionalization following a procedure prior described by Vernè et al. [30,31]. Briefly, specimens were first washed with acetone in ultrasonic bath for 5 minutes and then with ultrapure water for 5 minutes in ultrasonic bath, 3 times. After this washing step, glasses were functionalized using a 1 mg/mL or 5 mg/mL *P. pavonica* polyphenols solution (5 mL/specimen, resuspended in ultrapure water) by soaking technique 3 h at 37 °C in the dark. At the end of the soaking step, samples were gently washed twice in ultrapure water and dried in a laminar flow cabinet.

To achieve in situ reduction of silver nanoparticles (AgNPs) on the surface of functionalized glasses previously grafted with 1 mg/mL of *P. pavonica* extract, specimens were soaked 1 h at 37 °C in a 0.005 M silver nitrate ($AgNO_3$) aqueous solution in the dark prior to being finally washed in ultrapure water [21].

2.3.2. Specimens Surface Characterization

The Folin–Ciocalteau test was performed on the functionalized specimens to determine the total adhered phenol content [32].

The presence of molecules on the glass surfaces was also investigated also by means of X-ray photoelectron spectroscopy (XPS; PHI 5000 VersaProbe, Physical Electronics, Chanhassen, MN, USA) on samples functionalized with the 1 mg/mL solution before and after in situ reduction of AgNPs. Both survey spectra (for the determination of the chemical composition) and high-resolution spectra of the most important elements (C, O, and Ag to determine specific functional groups as well as the chemical state of silver) were acquired.

The precipitation of AgNPs after in situ Ag reduction was investigated by means of FE-SEM equipped with an EDS camera (FE-SEM-EDS, Supratum 40, Carl Zeiss, Oberkochen, Germany) after Pt surface sputter coating.

2.4. Antibacterial Evaluation

2.4.1. Strain

The orthopedic-infections-related, multi-drug resistant (MDR) certified biofilm former strain *S. aureus* (SA, ATCC 43300, purchased from the American Type Culture Collection, Manassas, MA, USA) was used to assay the specimens' antibacterial activity. SA was cultivated into selective blood agar medium (Sigma Aldrich, Milan, Italy); bacteria were cultivated at 37 °C until round colonies formed on the agar surface. Plates were maintained at 4 °C prior to experiments; fresh broth-cultures were prepared prior to each experiment by dissolving some colonies in 10 mL of Luria Bertani (LB) broth culture (Sigma Aldrich, Milan, Italy). Finally, bacteria concentration was adjusted until 1×10^5 cells/mL by diluting in fresh media until the optical density of 0.001 at 600 nm was reached as determined by a spectrophotometer (Victor, Packard Bell, Lainate, Italy).

2.4.2. Biofilm Formation

Sterile specimens were gently paced into a 12 multi-well plate using sterile tweezers avoiding any surface damage. Each specimen was submerged with 1 mL of the broth bacteria culture prepared as described in Section 2.5.1.; the plate was incubated for 90 minutes in agitation (120 rpm) at 37 °C to allow the separation between adherent biofilm cells and non-adherent floating planktonic cells (separation phase) [33,34]. Afterwards, supernatants containing planktonic cells were removed and replaced with 1 mL fresh media to cultivated surface-adhered biofilm cells (growth phase). Biofilms were grown at 37 °C for 1 to 3 days prior to evaluations [33,34].

2.4.3. Metabolic Evaluation

At each time-point, bacterial biofilm metabolic activity was evaluated by the colorimetric Alamar blue assay (alamarBlue®, Life Technologies, Milan, Italy) following the manufacturer's instructions. Briefly, specimens were gently moved to a new 12 multi-well plate and washed 3 times with sterile phosphate buffered saline (PBS, from Sigma, Milan, Italy) to remove non-adherent cells; then, specimens were submerged with 1 mL of the ready-to use Alamar blue solution and the plate was incubated at 37 °C in the dark for 5 h. Finally, 100 μL of supernatant was collected from each well, transferred to a black-bottom 96-well plate and the fluorescent signal was detected using a spectrophotometer (Victor, Packard Bell, Lainate, Italy) at a 590 nm wavelength. Results are expressed as relative fluorescence unit (RFU).

2.5. Cytotoxicity Evaluation

2.5.1. Cells

Human primary osteoblasts progenitors (hFOB 1.19, CRL-11372, ATCC, Manassas, MA, USA) were selected as test cells to evaluate specimens' cytocompatibility in vitro. hFOB cells were cultivated in MEM/F12 mix medium (50:50, Sigma, Milan, Italy) 10% fetal bovine serum (FBS, Sigma), 1% antibiotics, and 3 mg/mL neomycin (G418 salt, Sigma, Milan, Italy). Cells were cultivated until 80–90% confluence,

detached with trypsin/ethylene diamine triacetic acid solution (trypsin/EDTA, Sigma, Milan, Italy) and used for experiments.

2.5.2. Direct Metabolic Evaluation

Cells were cultivated in direct contact with the specimens' surface to reveal eventual toxic compounds on the coating [35]. Sterile specimens were gently placed into a 12 multi-well plate using sterile tweezers, avoiding any surface damage. Then, 2×10^4 cells/specimens were dropwise (100 µL) seeded directly onto specimens' surfaces and allowed to adhere for 2 h; afterwards, 1 mL of fresh medium was gently spotted into each well to fill specimens. Cells were cultivated for 1 to 3 days onto specimens' surfaces and viability was evaluated at each time point using the Alamar blue assay (alamarBlue®, Life Technologies, Milan, Italy) as previously described in Section 2.4.3. Results are expressed by means of RFU.

2.6. Statistical Analysis of Data

Data were analyzed using SPSS software (v25, IBM, New York, NY, USA) by means of one-way ANOVA followed by the Tukey' test as a post hoc analysis. Significance level was set to $p < 0.05$.

3. Results and Discussion

3.1. Polyphenols, Carotenoids, and Chlorophylls Quantification from P. pavonica Extract

Prior to undergoing CEL2 surface functionalization, the total polyphenol content in *P. pavonica* extract was evaluated by means of the Folin–Ciocalteu test to determine whether the selected source was sufficient to provide an adequate bulk of polyphenols. This step was performed as natural extracts often differ considerably from each other in terms of polyphenols content due to the different geographical origin. So, *P. pavonica* extract was expected to differ from previous sources of polyphenols we previously proposed [29]. Results confirmed that the selected *P. pavonica* algae was rich in polyphenols as the total amount resulted in 75.6 mg GAE/g DW (the polyphenols in the extract have the same redox activity of a gallic acid solution: 75.6 mg GAE/g in distilled water). By the same analysis, we determined that the carotenoids amount was quantified in 0.9 µg/g DW and that Chlorophyll b (Chl-b) was the most abundant pigment in *P. pavonica* extract (129.6 µg/g DW).

3.2. Specimens' Physico-Chemical Characterization

After analyzing the chemical features of the raw extract, we functionalized the bioactive CEL2 glass. The success of the entire procedure is based on different parameters that start from the extract stability that can be affected by pH variations. Accordingly, the pH of the applied *P. pavonica* solutions (1 and 5 mg/mL) was evaluated before and after the soaking step; the results are summarized in Table 1.

Table 1. *Padina pavonica* solutions pH evaluation before (pad) and after (CEL2 + pad) soaking.

Sample	pH
pad (1 mg/mL)	6.76
pad (5 mg/mL)	7.44
CEL2 + pad (1 mg/mL)	7.53 (± 0.06)
CEL2 + pad (5 mg/mL)	8.28 (± 0.04)

The starting pH of the *P. pavonica* solution was close to seven, which is less acidic than that recorded for other natural extracts such as gallic acid, grape polyphenols, and tea polyphenols that we previously investigated [29]. A moderate basification was detected after glass soaking due to the ion release from the glass surface; these variations in pH were less evident than that we previously observed for gallic acid, grape polyphenols, and tea polyphenols, thus demonstrating a higher stability of the grafting procedure [29]. A strong shift to a basic environment can favor both a further hydroxylation of the

glass and the oxidation of catechol groups of phenols to quinone groups [30]. As a further macroscopic confirmation of the extract stability, no color changes were recorded, nor for solutions, nor for samples after algae functionalization, thus suggesting that no significant changes in the pH occurred due to bioactive glass contact.

Once the surface functionalization was completed, the quantification of total polyphenols onto the CEL2 surface was verified by means of the Folin–Ciocalteau test. The results are reported in Table 2.

Table 2. CEL2 surface polyphenols amount after functionalization.

Sample	Polyphenols (GAE mg/mL)
CEL2 + pad (1 mg/mL)	0.001
CEL2 + pad (5 mg/mL)	0.001

As far as functionalized glass samples are concerned, about 0.001 mg/mL GAE was quantified by the Folin–Ciocalteau test. The Folin–Ciocalteau test is commonly used for the quantification of the total amount of polyphenols in solutions. We adapted the method [29,32] to solid surfaces. All the values can be considered as analogous samples of 1 cm^2 area and are comparable. Measurements were recorded on a small set of samples (n = 3) obtaining the same results (this is why standard deviation is not reported). This value is comparable with that previously obtained by functionalizing the CEL2 surface with grape skin extracts [29]. However, the final volume of grafted polyphenols seems to be independent of the concentration of the source solution (1 or 5 mg/mL of freeze-dried extract in ultrapure water), different from what we previously observed for grape and tea polyphenols. This difference can be associated with the different typologies of the molecules grafted onto the surface, which is worthy of further investigations. As the amount of polyphenols grafted on the surface did not increase the uptake solution concentration, further investigations were performed on glass samples functionalized with 1 mg/mL of *P. pavonica* solution.

Different from polyphenols functionalization, surface darkening was evidenced after AgNPs in situ reduction. As a confirmation of this macroscopic evidence, the atomic percentages of elements on the surface of bare CEL2, CEL2 + pad 1 mg/mL, and CEL2 + pad 1 mg/mL + Ag obtained by XPS survey analysis are reported in Table 3.

Table 3. Atomic percentages of elements from XPS survey analyses.

Element	CEL2	CEL2 + pad (1 mg/mL)	CEL2 + pad (1 mg/mL) + Ag
O	43.3	46.9	35.1
C	36.9	28	41.9
Si	13.5	12	8.0
Na	2.1	2	2.0
Ca	1.8	3.7	3.9
Al	1.4	–	–
Mg	0.9	7.5	4.8
Ag	–	–	3.3

No evident modifications of the chemical composition of the glass were detected after surface functionalization. This phenomenon can be ascribed to the moderate amount of biomolecules grafted and to the fact that they mainly constituted of carbon and oxygen, which are already present in the glass and on its surface due to unavoidable atmospheric contaminations.

The appearance of silver was clearly detected after in situ reduction, confirming the surface ability to facilitate Ag precipitation; this behavior and the amount of silver are in accordance with the results we previously obtained on the same glass functionalized with gallic acid, grape, and tea polyphenols [21]. The high-resolution spectra of carbon and oxygen regions for bare and *P. pavonica*-polyphenols-functionalized CEL2 samples are reported in Figure 1.
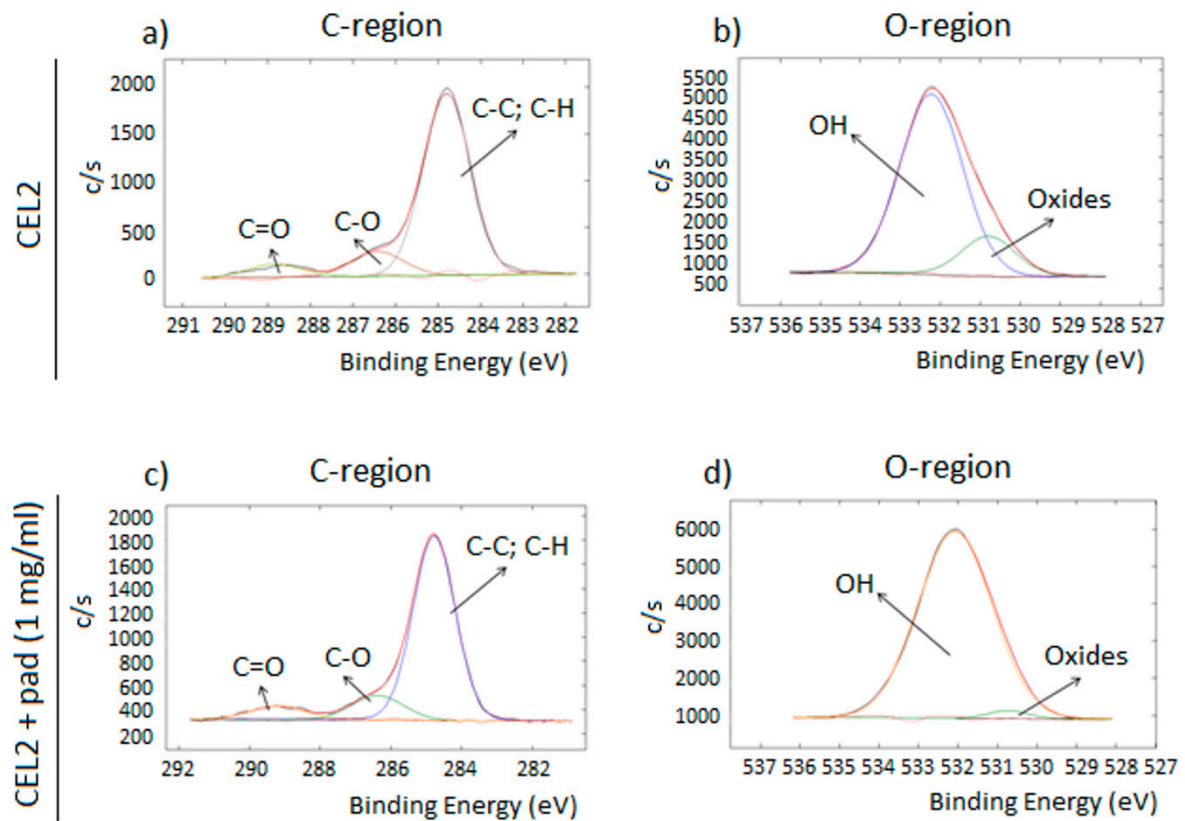
Figure 1. High resolution XPS spectra of (**a**,**c**) carbon (C-region) and (**b**,**d**) oxygen (O-region) for bare (CEL2) and *P. pavonica* extract grafted (CEL2 + pad (1 mg/mL) CEL2 specimens.

No significant differences were detected between bare (CEL2) and functionalized (CEL2 + pad 1 mg/mL) bioactive glass in the carbon region (Figure 1a,c). An increase in the OH signal was highlighted in the oxygen region for the functionalized specimens. This increase can be attributed to the OH groups belonging to polyphenols as previously described [29].

Once AgNPs were introduced into the CEL2 surfaces containing polyphenols, the typical Ag signal was clearly detected by high resolution spectra as a confirmation of the corrected co-grafting between *P. pavonica* polyphenols and AgNPs. The high-resolution spectrum of silver detected on CEL2 + pad (1 mg/mL) +Ag is reported in Figure 2.
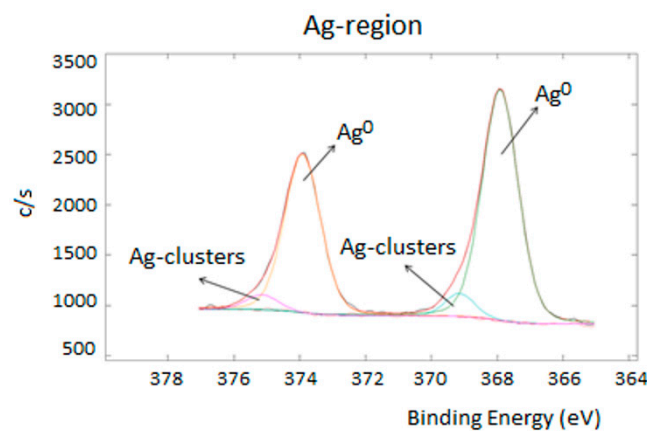

Figure 2. High resolution XPS spectrum of the Ag region for CEL2 + pad (1 mg/mL) +Ag.

The main doublet was detected at 367.92–373.92 eV, close to the typical binding energy of metallic silver [36,37]; these findings are in line to the hypothesis of an in situ reduction induced on the glass surface by algae polyphenols, in a similar manner as previously observed on bioactive glasses functionalized with natural polyphenols [33]. Then, a second small doublet was detected at 369.15–375.15, which can be probably associated with the presence of silver clusters [36]. To verify this hypothesis, FE-SEM images of CEL2 + pad (1 mg/mL) + Ag specimens were collected and reported in Figure 3.
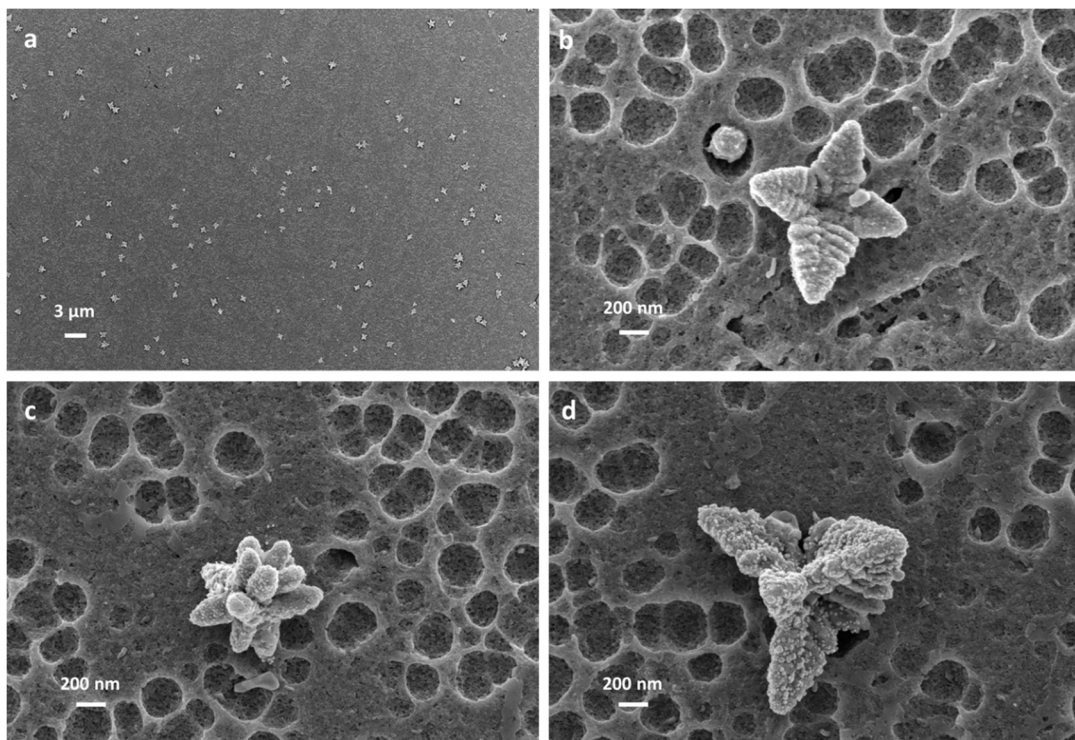
Figure 3. FE-SEM observations of CEL2 + pad (1 mg/mL) + Ag. (**a**) Low magnification overview of surface; (**b**–**d**) Ag precipitates as dendrimeric nanoflowers and holes on the glass surface due to reaction in the functionalization media (higher magnification).

Looking at the images, a uniform distribution of precipitates was observed all over the surface (Figure 3a). Their morphologies are similar and can be defined as dendrimeric nanoflowers (Figure 3b–d) with dimensions varying around 400–800 nm. It is possible to speculate that they are derived from nanometric particles aggregation as previously suggested by the presence of silver clusters detected by XPS. Some holes were also observed on the surface and can be ascribed to the surface reaction of the glass (ion release and partial dissolution associated with the bioactivity mechanisms) in the functionalization media.

As a further confirmation of this hypothesis, EDS analyses (Figure 4) confirmed that observed precipitates were mainly constituted of silver. Silver signals were only detected within the precipitates whereas no other signals were observed when analyzing other surface areas. This result is in accordance with the metallic nature of silver, which selectively precipitates in metallic form due to the reducing action of surface grafted polyphenols on Ag ions within the solution.
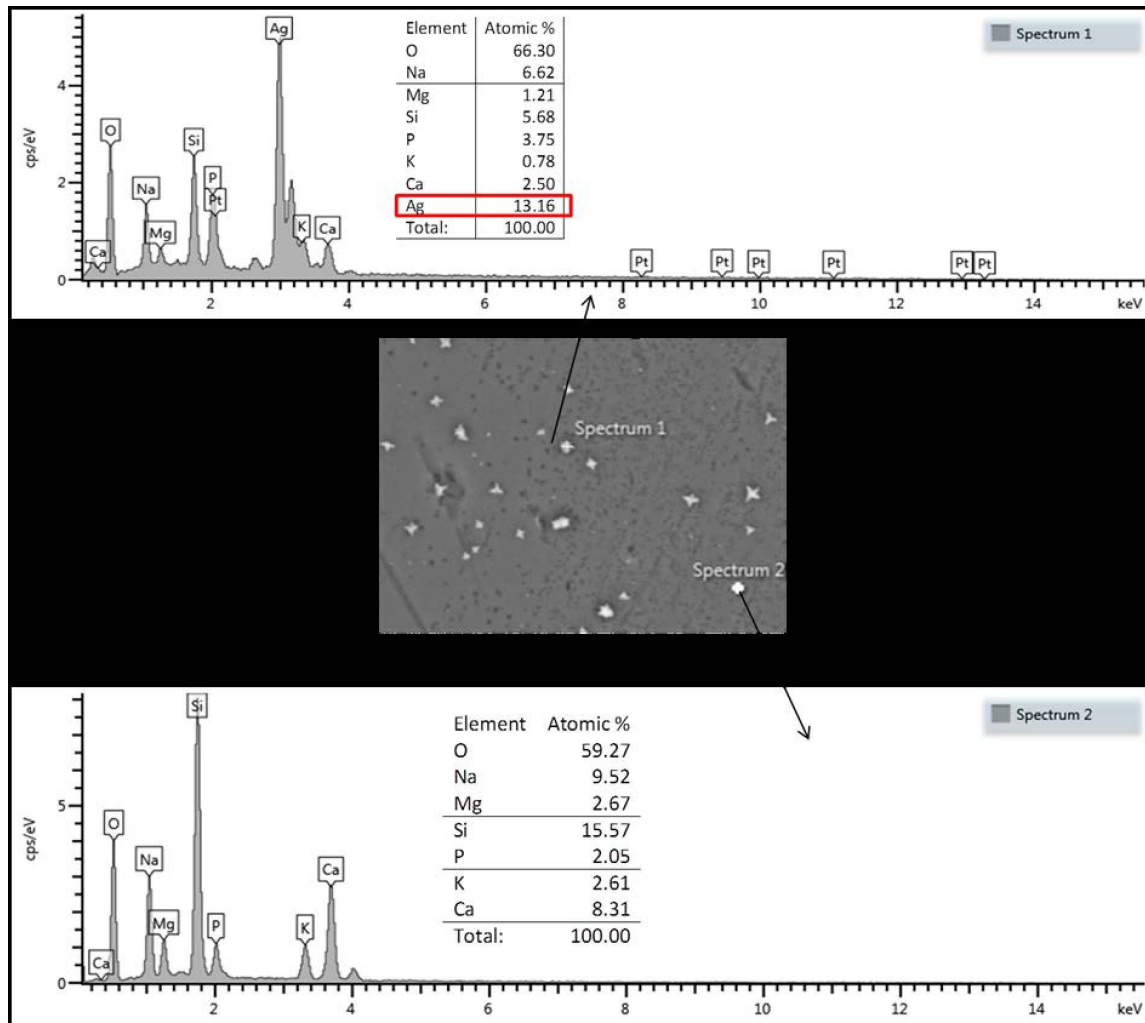
Figure 4. EDS analyses on CEL2 + pad (1 mg/mL) + Ag.

3.3. Antibacterial Evaluation

The results concerning antibacterial activity obtained by contaminating doped and control specimens directly in contact with 1×10^5 cells/mL *Staphylococcus aureus* suspension are reported in Figure 5. Here, we selected a certified multi-drug resistant strain (ATCC 43300) to test specimens' antibacterial performance towards bacteria resistant to conventional drug treatments.

The use of polyphenols from *P. pavonica* extract only (1 mg/mL, named CEL2 + pad) was not sufficient to determine a significant decrease in bacteria metabolism ($p > 0.05$) at each tested time-points in comparison with untreated CEL2 controls. Conversely, when silver nanoparticles (1 mg/mL, labelled CEL2 + pad + Ag) were coupled with the algae extract, a strong significant decrease was observed after 24 (Figure 5a) and 48 (Figure 5b) h, whereas the effect decreased after 72 h (Figure 5c), probably due to the limited amount of antibacterial compounds still available for release. The amounts of grafted Ag ions and polyphenols are not unlimited and thus the efficacy is strongly related to the release period. So, our hypothesis is that once all the polyphenols and the Ag ions are completely delivered into the medium, their effects conclude and the bacteria that survived until that moment started to proliferate again. This behavior is analogous to that we previously observed for bioactive glasses functionalized with grape and tea polyphenols—the presence of the polyphenols alone is not able to induce a strong antibacterial behavior but the in situ reduction of silver nanoparticles significantly increases this activity.

The *P. pavonica* polyphenols extract + AgNPs combination was here tested to improve the antibacterial properties of the bioactive CEL2 glass for the first time, to the best of our knowledge. The obtained results are encouraging because the combined effect of these two antibacterial agents was effective at significantly reducing *S. aureus* viability onto bioactive glasses. The hypothesis at the base of this combination was related to the possibility of coupling different broad-range antibacterial activities derivates from a natural compound and a broad range antibacterial metal in terms of nanoparticles.

Ag is known to be effective towards a large class of both Gram-positive and Gram-negative strains due to its ability to anchor to the bacterial cell membrane by electrostatic reaction; as such, bacteria die due to the irreversible membrane damage [38,39]. Ag was demonstrated to be able to trigger the formation of free ROS that leads to a strong increase in the microenvironment oxidative stress. This condition causes unrepairable damage to bacteria by directly targeting their DNA, thus irreversibly stopping the replication cycle, causing bacterial death [38,39].

Differently, the role of polyphenols in counteracting bacterial infection is less understood. The more accredited hypothesis is related to the possibility that polyphenols can link bacteria membrane phospholipids [40,41]; once this interaction occurs, the integrity of the membrane lipid bilayer is irredeemably compromised, thus leading to an increase in permeability, a loss of membrane fluidity, and an impairment of ions inside/outside transportation [40,41]. All these conditions are not compatible with correct metabolism, thus leading to bacteria death.
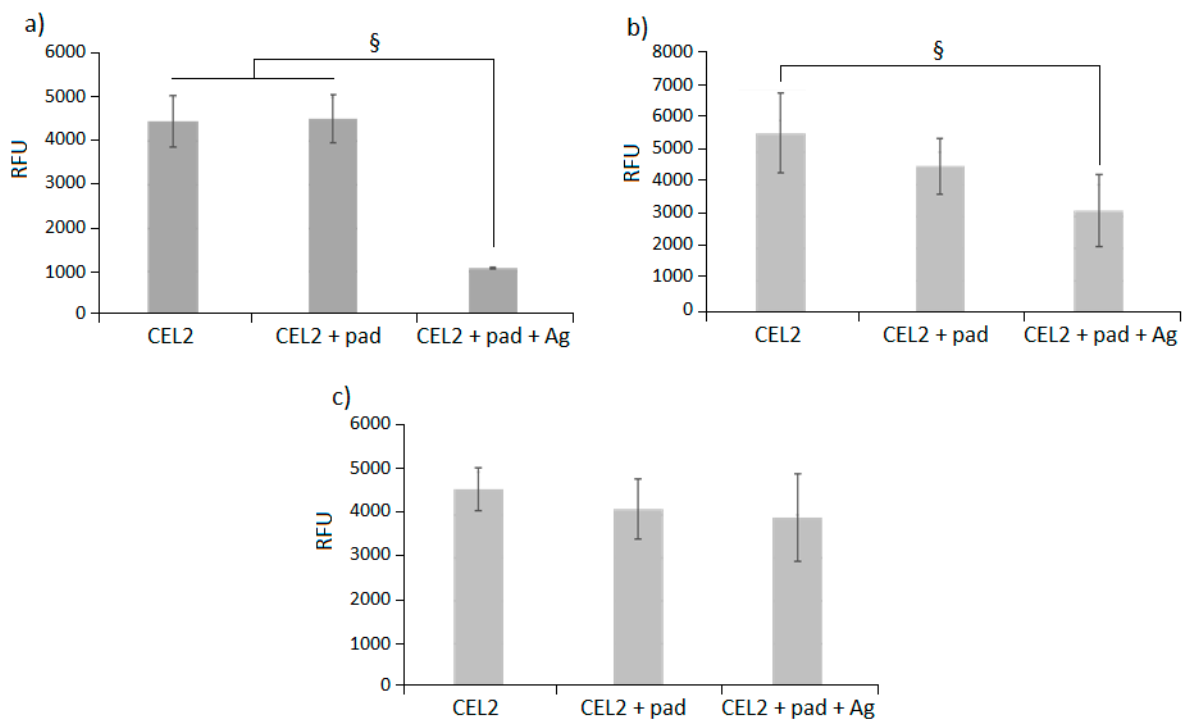

Figure 5. Specimens' antibacterial activity in direct contact with *S. aureus* biofilm for (**a**) 24, (**b**) 48, and (**c**) 72 h. The doping with algae extract only (CEL2 + pad) was not effective at decreasing bacteria viability ($p > 0.05$) in comparison with untreated controls (CEL2). The introduction of silver in combination with extract (CEL2 + pad + Ag) produced a decrease in bacteria metabolism that was significant after 24 and 48 h of cultivation (c, $p < 0.05$, indicated by the §) in comparison to both CEL2 and CEL2 + pad. The effect decreased after 72 h, probably due to saturation. Bars represent means and standard deviations; data are expressed as RFU.

According to this evidence, despite a more evident role of silver in comparison with polyphenols, we hypothesize that the obtained results are due to a combined activity that potentially irreversibly damages the bacteria membrane. This effect seems to be attractive, as it is not dependent on the Gram-positive or negative classification of the strain; moreover, it involves so many pathways (oxidative stress, DNA replication, membrane integrity, and ions trafficking) that bacteria may not easily develop resistance to all these mechanisms, thus making the treatment probably effective toward most bacterial strains.

From the materials point of view, the presence of polyphenols can have a double effect on the surface modification: acting as reducing agents to catalyze the precipitation of antibacterial silver nanoparticles and, imparting other properties to the surface specific to polyphenols (e.g., antioxidant, anti-inflammatory, bone stimulating, and anti-cancer) to make the surface multifunctional.

3.4. Cytocompatibility Evaluation

The results obtained by seeding cells directly in contact with doped and control specimens are shown in Figure 6. In general, the doping realized with algae extract only (1 mg/mL, called CEL2 + pad) did not have any toxic effect on the bioactive glass as results were comparable with controls (CEL2) at each time point ($p > 0.05$). Differently, the combination of the extract and silver nanoparticles (1 mg/mL, called CEL2 + pad + Ag) produced a decrease in cell viability that was evident, in particular, after three days' cultivation (Figure 6c). The results are significant in comparison with both CEL2 control and CEL2 + pad ($p < 0.05$, indicated by §). Accordingly, looking at the cell metabolism as a function of time (Figure 6d), values were increasing for CEL2 and CEL2 + pad specimens, thus prompting us to hypothesize that cell number increased during the experimental time-points. Conversely, results from CEL2 + pad + Ag showed a stationary plateau phase between 24 and 48 h and a slight decrease from 48 to 72 h (Figure 6c).

The obtained results can generally be considered as being in agreement with previous literature. The bare CEL2 bioactive glasses were considered as a control due to their well-known cytocompatibility towards osteoblasts. They can be considered as superior in terms of bioactivity in comparison with glass based on the SiO_2–CaO–Na_2O–Al_2O_3 system (named SCNA) that were previously applied to test polyphenols and silver antibacterial properties [29]. They were shown to be affective in supporting primary osteoblasts colonization and proliferation through their ordered mesoporous channels configuration that permits proper transportation of nutrients as well as released ions [7–9]. The subsequently formed HCA layer serves as an ideal environment for the osteoblast's growth, thus promoting bone self-healing [7–9].

The introduction of polyphenols from *P. pavonica* algae extract did not decrease cells metabolism, thus demonstrating cytocompatibility. Besides their recognized antibacterial activity, polyphenols are known to be effective at free radicals scavenging [42–45]. In cell cultures, they can directly interact with cell cytoskeletons through the phenolic hydroxyl groups [42–44]. Due to this tight interaction, polyphenols seem to be effective at protecting cells from damage due to oxidative stress, thus supporting proliferation [46].

However, when the algae extract was coupled with silver nanoparticles, we detected a significant increase in specimens' cytotoxicity. As the extract itself is not toxic as previously debated, we speculate that this toxic effect can be attributed mainly to the silver (Ag). Ag is known to be a potential toxic element for cells [47–50]; it can trigger the formation of ROS by preventing intracellular antioxidants and cause DNA damage that results in cell death [47,48]. This mechanism can be initiated by the Ag uptake by the cellular clathrin-dependent endocytosis and micropinocytosis; as a consequence, physiological impairment can be achieved due to the ROS increase [49,50].

Another explanation of Ag potential toxicity is due to the employment of AgNPs [51–55]. Due to their nano-size, AgNPs can easily interact with cellular organelles, producing a lack of functioning due to direct contact or accumulation [51–55].
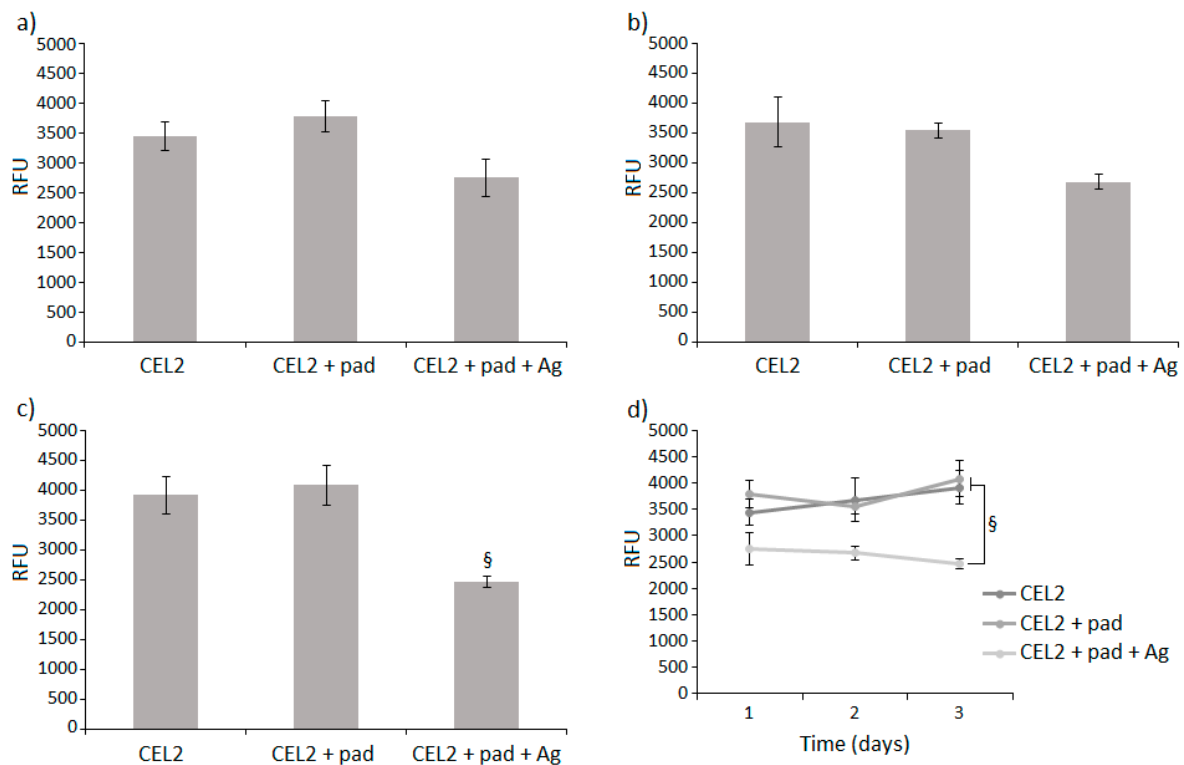
Figure 6. Specimens' cytocompatibility in direct contact with hFOB cells for (**a**) 24, (**b**) 48, and (**c**) 72 h. The doping with algae extract only (CEL2 + pad) did not introduce any toxic effect, as results were comparable ($p > 0.05$) with untreated controls (CEL2). The introduction of silver in combination with extract (CEL2 + pad + Ag) produced a decrease of cells metabolism that was significant after 72 h of cultivation (c, $p < 0.05$ indicated by the §) in comparison with both CEL2 and CEL2 + pad. (**d**) Accordingly, cells metabolism decreased during the 72 h. (Bars represent means and standard deviations; data are expressed as RFU.

4. Conclusions

The combined polyphenols from *P. pavonica* algae and silver nanoparticles (AgNPs) surface doping of bioactive glasses CEL2 was successfully achieved using an in situ reduction technique. The specimens' chemical-physical analysis confirmed that both polyphenols and AgNPs were homogeneously spread onto the glass surface. The obtained composites showed a strong ability to prevent *S. aureus* biofilm contamination due to a combined activity mainly targeted toward the bacteria membrane. However, a certain specimen toxicity was observed toward human progenitor cells.

The proposed procedure for surface modification allows the tailoring of the silver content, so in the future, the amount of silver should be reduced to balance antibacterial activity and biocompatibility.

References

1. Collignon, A.M.; Lesieur, J.; Vacher, C.; Chaussain, C.; Rochefort, G.Y. Strategies developed to induce, direct, and potentiate bone healing. *Front. Physiol.* **2017**, *8*, 927. [CrossRef] [PubMed]
2. Martin, V.; Bettencourt, A. Bone regeneration: Biomaterials as local delivery systems with improved osteoinductive properties. *Mater. Sci. Eng. C Mater. Biol. Appl.* **2018**, *82*, 363–371. [CrossRef] [PubMed]

3. Lu, H.; Liu, Y.; Guo, J.; Wu, H.; Wang, J.; Wu, G. Biomaterials with antibacterial and osteoinductive properties to repair infected bone defects. *Int. J. Mol. Sci.* **2016**, *17*, 334. [CrossRef] [PubMed]

4. Wilson, J.; Low, S.B. Bioactive ceramics for periodontal treatment: Comparative studies in the Patus monkey. *J. Appl. Biomater. Funct. Mater.* **1992**, *3*, 123–129. [CrossRef] [PubMed]

5. Hench, L.L.; Wilson, J. Surface-active biomaterials. *Science* **1984**, *226*, 630. [CrossRef] [PubMed]

6. Hench, L.L. The story of Bioglass. *J. Mater. Sci. Mater. Med.* **2006**, *17*, 967–978. [CrossRef]

7. Newby, P.J.; El-Gendy, R.; Kirkham, J.; Yang, X.B.; Thompson, I.D.; Boccaccini, A.R. Ag-doped 45S5 Bioglass®-based bone scaffolds by molten salt ion exchange: Processing and characterisation. *J. Mater. Sci. Mater. Med.* **2011**, *22*, 557–569. [CrossRef]

8. Caridade, S.G.; Merino, E.G.; Alves, N.M.; Mano, J.O.F. Bioactivity and viscoelastic characterization of chitosan/bioglass® composite membranes. *Macromol. Biosci.* **2012**, *12*, 1106–1113. [CrossRef]

9. Hench, L.L.; Polak, J.M. Third-generation biomedical materials. *Science* **2002**, *295*, 1014–1017. [CrossRef]

10. Vernè, E.; Ferraris, S.; Vitale-Brovarone, C.; Cochis, A.; Rimondini, L. Bioactive glass functionalized with alkaline phosphatase stimulates bone extracellular matrix deposition and calcification in vitro. *Appl. Surf. Sci.* **2014**, *313*, 372–381. [CrossRef]

11. De Jesus Raposo, M.F.; de Morais, A.M.; de Morais, R.M. Marine polysaccharides from algae with potential biomedical applications. *Mar. Drugs* **2015**, *13*, 2967–3028. [CrossRef] [PubMed]

12. Senthilkumar, K.; Manivasagan, P.; Venkatesan, J.; Kim, S.K. Brown seaweed fucoidan: Biological activity and apoptosis, growth signaling mechanism in cancer. *Int. J. Biol. Macromol.* **2013**, *60*, 366–374. [CrossRef] [PubMed]

13. Kelman, D.; Posner, E.K.; McDermid, K.J.; Tabandera, N.K.; Wright, P.R.; Wright, A.D. Antioxidant activity of Hawaiian marine algae. *Mar. Drugs* **2012**, *10*, 403–416. [CrossRef] [PubMed]

14. Jose, G.M.; Radhakrishnan, A.; Kurup, G.M. Antioxidant and antimitotic activities of sulfated polysaccharide from marine brown algae *Padina tetrastromatica*. *J. Phytol.* **2015**, *7*, 39. [CrossRef]

15. El-Aty, A.M.A.; Mohamed, A.A.; Samhan, F.A. In vitro antioxidant and antibacterial activities of two fresh water Cyanobacterial species, *Oscillatoria agardhii* and *Anabaena sphaerica*. *JAPS* **2014**, *4*, 69–75. [CrossRef]

16. Cheng, Y.C.; Sheen, J.M.; Hu, W.L.; Hung, Y.C. Polyphenols and oxidative stress in atherosclerosis-related ischemic heart disease and stroke. *Oxid. Med. Cell. Longev.* **2017**, *2017*, 8526438. [CrossRef] [PubMed]

17. Cushnie, T.P.T.; Hamilton, V.E.S.; Chapman, D.G.; Taylor, P.W.; Lamb, A.J. Aggregation of Staphylococcus aureus following treatment with the antibacterial flavonol galangin. *JAPS* **2007**, *103*, 1562–1567. [CrossRef] [PubMed]

18. Dua, A.; Garg, G.; Mahajan, R. Polyphenols, flavonoids and antimicrobial properties of methanolic extract of fennel (*Foeniculum vulgare* Miller). *Eur. J. Exp. Biol.* **2013**, *3*, 203–208.

19. Alhussaini, M.S.; Saadabi, A.M.; Alghonaim, M.I.; Ibrahim, K.E. An evaluation of the Antimicrobial activity of *Commiphora myrrha* Nees (Engl.) oleo-gum resins from Saudi Arabia. *J. Med. Sci.* **2015**, *15*, 198–203. [CrossRef]

20. Sahoo, S.S.; Shukla, S.; Nandy, S.; Sahoo, H.B. Synthesis of novel coumarin derivatives and its biological evaluations. *Eur. J. Exp. Biol.* **2012**, *2*, 899–908.

21. Ferraris, S.; Miola, M.; Cochis, A.; Azzimonti, B.; Rimondini, L.; Prenesti, E.; Vernè, E. In situ reduction of antibacterial silver ions to metallic silver nanoparticles on bioactive glasses functionalized with polyphenols. *Appl. Surf. Sci.* **2017**, *396*, 461–470. [CrossRef]

22. Miola, M.; Cochis, A.; Kumar, A.; Arciola, C.; Rimondini, L.; Verné, E. Copper-doped bioactive glass as filler for PMMA-based bone cements: Morphological, mechanical, reactivity, and preliminary antibacterial characterization. *Materials* **2018**, *11*, 961. [CrossRef] [PubMed]

23. Hamouda, T.; Myc, A.; Donovan, B.; Shih, A.Y.; Reuter, J.D.; Baker, J.R. A novel surfactant nanoemulsion with a unique non-irritant topical antimicrobial activity against bacteria, enveloped viruses and fungi. *Microbiol. Res.* **2001**, *156*, 1–7. [CrossRef]

24. Russel, A.D.; Hugo, W.B. Antimicrobial activity and action of silver. *Prog. Med. Chem.* **1994**, *31*, 351–370. [CrossRef]

25. Sondi, I.; Salopek-Sondi, B. Silver nanoparticles as antimicrobial agent: A case study on *E. coli* as a model for Gram-negative bacteria. *J. Colloid Interface Sci.* **2004**, *275*, 177–182. [CrossRef] [PubMed]

26. Zhang, T.; Wang, L.; Chen, Q.; Chen, C. Cytotoxic potential of silver nanoparticles. *Yonsei Med. J.* **2014**, *55*, 283–291. [CrossRef] [PubMed]

27. Scalbert, A.; Monties, B.; Janin, G. Tannins in wood: Comparison of different estimation methods. *J. Agric. Food Chem.* **1989**, *37*, 1324–1329. [CrossRef]

28. Sumanta, N.; Haque, C.I.; Nishika, J.; Suprakash, R. Spectrophotometric analysis of chlorophylls and carotenoids from commonly grown fern species by using various extracting solvents. *Res. J. Chem. Sci.* **2014**, *2231*, 606. [CrossRef]

29. Cazzola, M.; Corazzari, I.; Prenesti, E.; Bertone, E.; Vernè, E.; Ferraris, S. Bioactive glass coupling with natural polyphenols: Surface modification, bioactivity and antioxidant ability. *Appl. Surf. Sci.* **2016**, *367*, 237–248. [CrossRef]

30. Verne, E.; Vitale-Brovarone, C.; Bui, E.; Bianchi, C.L.; Boccaccini, A.R. Surface functionalization of bioactive glasses. *J. Biomed. Mater. Res. Part A* **2009**, *90*, 981–992. [CrossRef]

31. Verné, E.; Ferraris, S.; Vitale-Brovarone, C.; Spriano, S.; Bianchi, C.L.; Naldoni, A.; Morra, M.; Cassinelli, C. Alkaline phosphatase grafting on bioactive glasses and glass ceramics. *Acta Biomater.* **2010**, *6*, 229–240. [CrossRef] [PubMed]

32. Ferraris, S.; Zhang, X.; Prenesti, E.; Corazzari, I.; Turci, F.; Tomatis, M.; Vernè, E. Gallic acid grafting to a ferrimagnetic bioactive glass-ceramic. *J. Non-Cryst Solids* **2016**, *432*, 167–175. [CrossRef]

33. Ferraris, S.; Giachet, F.T.; Miola, M.; Bertone, E.; Varesano, A.; Vineis, C.; Cochis, A.; Sorrentino, R.; Rimondini, L.; Spriano, S. Nanogrooves and keratin nanofibers on titanium surfaces aimed at driving gingival fibroblasts alignment and proliferation without increasing bacterial adhesion. *Mater. Sci. Eng. C Mater. Biol. Appl.* **2017**, *76*, 1–12. [CrossRef] [PubMed]

34. Bonifacio, M.A.; Cometa, S.; Cochis, A.; Gentile, P.; Ferreira, A.M.; Azzimonti, B.; Procino, G.; Ceci, E.; Rimondini, L.; De Giglio, E. Antibacterial effectiveness meets improved mechanical properties: Manuka honey/gellan gum composite hydrogels for cartilage repair. *Carbohydr. Polym.* **2018**, *198*, 462–472. [CrossRef] [PubMed]

35. Cochis, A.; Rimondini, L.; Pourroy, G.; Stanic, V.; Palkowski, H.; Carradò, A. Biomimetic calcium–phosphates produced by an auto-catalytic route on stainless steel 316L and bio-inert polyolefin. *RSC Adv.* **2013**, *3*, 11255–11262. [CrossRef]

36. Galindo, R.E.; Benito, N.; Palacio, C.; Cavaleiro, A.; Carvalho, S. Ag+ release inhibition from ZrCN–Ag coatings by surface agglomeration mechanism: Structural characterization. *J. Phys. D Appl. Phys.* **2013**, *46*, 325303. [CrossRef]

37. Ferraris, M.; Ferraris, S.; Miola, M.; Perero, S.; Balagna, C.; Verne, E.; Gautier, G.; Manfredotti, C.; Battiato, A.; Vittone, E.; et al. Effect of thermal treatments on sputtered silver nanocluster/silica composite coatings on soda-lime glasses: Ionic exchange and antibacterial activity. *J. Nanopart. Res.* **2012**, *14*, 1287. [CrossRef]

38. Maliszewska, I.; Sadowski, Z. Synthesis and antibacterial activity of silver nanoparticles. *J. Phys. Conf. Ser.* **2009**, *146*, 012024. [CrossRef]

39. Le Ouay, B.; Stellacci, F. Antibacterial activity of silver nanoparticles: A surface science insight. *Nano Today* **2015**, *10*, 339–354. [CrossRef]

40. Papuc, C.; Goran, G.V.; Predescu, C.N.; Nicorescu, V.; Stefan, G. Plant polyphenols as antioxidant and antibacterial agents for shelf-life extension of meat and meat products: Classification, structures, sources, and action mechanisms. *Compr. Rev. Food Sci.* **2017**, *16*, 1243–1268. [CrossRef]

41. Sun, Y.; Hung, W.C.; Chen, F.Y.; Lee, C.C.; Huang, H.W. Interaction of tea catechin (−)-epigallocatechin gallate with lipid bilayers. *Biophys. J.* **2009**, *96*, 1026–1035. [CrossRef] [PubMed]

42. Shavandi, A.; Bekhit, A.E.D.A.; Saeedi, P.; Izadifar, Z.; Bekhit, A.A.; Khademhosseini, A. Polyphenol uses in biomaterials engineering. *Biomaterials* **2018**, *167*, 91–106. [CrossRef] [PubMed]

43. Surget, G.; Roberto, V.P.; Le Lann, K.; Mira, S.; Guérard, F.; Laizé, V.; Poupart, N.; Cancela, M.L.; Stiger-Pouvreau, V. Marine green macroalgae: A source of natural compounds with mineralogenic and antioxidant activities. *J. Appl. Phycol.* **2017**, *29*, 575–584. [CrossRef]

44. Kurt, O.; Özdal-Kurt, F.; Akçora, C.M.; Özkut, M.; Tuğlu, M.I. Neurotoxic, cytotoxic, apoptotic and antiproliferative effects of some marine algae extracts on the NA2B cell line. *Biotech. Histochem.* **2018**, *93*, 59–69. [CrossRef] [PubMed]

45. Upadhyay, S.; Dixit, M. Role of polyphenols and other phytochemicals on molecular signaling. *Oxid. Med. Cell. Longev.* **2015**, *2015*, 504253. [CrossRef] [PubMed]

46. Fawcett, D.; Verduin, J.J.; Shah, M.; Sharma, S.B.; Poinern, G.E.J. A review of current research into the biogenic synthesis of metal and metal oxide nanoparticles via marine algae and seagrasses. *J. Nanosci.* **2017**, *2017*, 8013850. [CrossRef]

47. Skalska, J.; Strużyńska, L. Toxic effects of silver nanoparticles in mammals—Does a risk of neurotoxicity exist? *Folia Neuropathol.* **2015**, *53*, 281. [CrossRef] [PubMed]

48. Ahmed, L.B.; Milić, M.; Pongrac, I.M.; Marjanović, A.M.; Mlinarić, H.; Pavičić, I.; Gajović, S.; Vrček, I.V. Impact of surface functionalization on the uptake mechanism and toxicity effects of silver nanoparticles in HepG2 cells. *Food Chem. Toxicol.* **2017**, *107*, 349–361. [CrossRef]

49. Nayak, D.; Minz, A.P.; Ashe, S.; Rauta, P.R.; Kumari, M.; Chopra, P.; Nayak, B. Synergistic combination of antioxidants, silver nanoparticles and chitosan in a nanoparticle-based formulation: Characterization and cytotoxic effect on MCF-7 breast cancer cell lines. *J. Colloid Interface Sci.* **2016**, *470*, 142–152. [CrossRef] [PubMed]

50. Saallah, S.; Lenggoro, I.W. Nanoparticles carrying biological molecules: Recent advances and applications. *Kona Powder Part J.* **2018**, *35*. [CrossRef]

51. Xu, L.Q.; Neoh, K.G.; Kang, E.T. Natural polyphenols as versatile platforms for material engineering and surface functionalization. *Prog. Polym. Sci.* **2018**, *87*, 165–196. [CrossRef]

52. Yedurkar, S.; Maurya, C.; Mahanwar, P. Biosynthesis of Zinc Oxide Nanoparticles Using Ixora Coccinea Leaf Extract—A Green Approach. *OJSTA* **2016**, *5*. [CrossRef]

53. Moulton, M.C.; Braydich-Stolle, L.K.; Nadagouda, M.N.; Kunzelman, S.; Hussain, S.M.; Varma, R.S. Synthesis, characterization and biocompatibility of "green" synthesized silver nanoparticles using tea polyphenols. *Nanoscale* **2010**, *2*, 763–770. [CrossRef] [PubMed]

54. Sheikholeslami, S.; Mousavi, S.E.; Ashtiani, H.R.A.; Doust, S.R.H.; Rezayat, S.M. Antibacterial activity of silver nanoparticles and their combination with zataria multiflora essential oil and methanol extract. *Jundishapur J. Microbiol.* **2016**, *9*, e36070. [CrossRef] [PubMed]

55. Matei, P.; Martín-Gil, J.; Michaela Iacomi, B.; Pérez-Lebeña, E.; Barrio-Arredondo, M.; Martín-Ramos, P. Silver nanoparticles and polyphenol inclusion compounds composites for *Phytophthora cinnamomi* mycelial growth inhibition. *Antibiotics* **2018**, *7*, 76. [CrossRef] [PubMed]